



NRC Publications Archive Archives des publications du CNRC

Foam-coated MIM gives new edge to titanium implants

Baril, Éric; Lefebvre, Louis-Philippe; Thomas, Yannig; Ilinca, Florin

This publication could be one of several versions: author's original, accepted manuscript or the publisher's version. /
La version de cette publication peut être l'une des suivantes : la version prépublication de l'auteur, la version
acceptée du manuscrit ou la version de l'éditeur.

For the publisher's version, please access the DOI link below. / Pour consulter la version de l'éditeur, utilisez le lien
DOI ci-dessous.

Publisher's version / Version de l'éditeur:

[http://dx.doi.org/10.1016/S0026-0657\(08\)70125-5](http://dx.doi.org/10.1016/S0026-0657(08)70125-5)

Metal Powder Report, 63, 8, pp. 46-55, 2008

NRC Publications Record / Notice d'Archives des publications de CNRC:

<http://nparc.cisti-icist.nrc-cnrc.gc.ca/npsi/ctrl?action=rtdoc&an=11707330&lang=en>

<http://nparc.cisti-icist.nrc-cnrc.gc.ca/npsi/ctrl?action=rtdoc&an=11707330&lang=fr>

Access and use of this website and the material on it are subject to the Terms and Conditions set forth at

http://nparc.cisti-icist.nrc-cnrc.gc.ca/npsi/jsp/nparc_cp.jsp?lang=en

READ THESE TERMS AND CONDITIONS CAREFULLY BEFORE USING THIS WEBSITE.

L'accès à ce site Web et l'utilisation de son contenu sont assujettis aux conditions présentées dans le site

http://nparc.cisti-icist.nrc-cnrc.gc.ca/npsi/jsp/nparc_cp.jsp?lang=fr

LISEZ CES CONDITIONS ATTENTIVEMENT AVANT D'UTILISER CE SITE WEB.

Contact us / Contactez nous: nparc.cisti@nrc-cnrc.gc.ca.



Fiche d'information et d'autorisation pour documents internes, externes et conférences



Auteurs

Auteur principal pour l'IMI

Nom	Prénom	Centre financ.	Centre de coût	Commande interne	Signature	Date sign.	Premier auteur publication
Baril	E.	505000	505200		<i>[Signature]</i>	27/01/09	*

Autres auteurs

Externe

Lefebvre	L.P.	505000	505200		<i>[Signature]</i>	27/01/09	
Thomas	Y.	505000	505200		<i>[Signature]</i>	26/01/09	
Ilinca	F.	504000	504500		<i>[Signature]</i>	30/01/09	

* Je certifie, en tant que premier auteur, que j'ai vérifié avec le(s) partenaire(s) qu'il(s) n'a (n'ont) pas d'objection à ce document.

Document

Titre

"Foam-coated MIM gives new edge to titanium implants"

Statut de distribution Confidentiel (aucune distribution) Restreint Général

Type

- Sommaire (abstract)** Écrit final à suivre : Oui_Yes Non_No Si oui, date : _____
 Rapport Technique Industriel de service
 Autre _____
 Document soumis pour publication

Si un **sommaire (abstract)** a été soumis précédemment, veuillez indiquer les numéros :

IMI _____ CNRC _____ CNRC _____

À présenter dans le cadre de :

Date de la conférence : _____ Lieu : _____

À paraître dans : _____ Date : _____

Statut de publication

À être complété par votre adjointe. Veuillez l'aviser lorsque l'information sera disponible.

- Revue ou livre avec comité de lecture
 Procès-verbal de conférence avec comité de lecture
 Procès-verbal de conférence sans comité de lecture
 Autre

Date de publication	Année cal. publication
2008-09-01	2008

Paru dans (vol. pp) : Metal Powder Report, Volume 63, Issue 8, September 2008, Pages 46-50, 52, 54-55

Autres informations

Partenaires : _____
 Déclaration d'invention : Oui_Yes Non_No Date : _____
 Demande de brevet déposée : Oui_Yes Non_No Pays : _____
 Si non, explications : _____

Approbations

[Signature] _____ *[Signature]* _____ *[Signature]* _____
 Signature Date Signature Date Signature Date
 Chef de groupe 12/02/09 Directeur de section 06/05/09 Directeur général 06-06-09

Numéro IMI 2009 - 119651 - G CNRC 51095

Foam-coated MIM gives new edge to titanium implants

Titanium's characteristics of lightness combined with strength and compatibility with human tissue makes it an ideal metal for medical implants. When manufactured in porous forms, bone integration is encouraged giving long-term stability. Researchers in Canada have been looking at dental implants that have a dense titanium core and a porous foam composite coat...

The biocompatibility of titanium (Ti) and titanium alloys has been proven in many experimental and clinical investigations. Those materials are now standard materials for the production of biomedical implants and are widely used in various dental and orthopaedic applications [1,2].

The influence of surface topography on cell adherence and morphogenesis has been widely reported and since the mid 1980s, interest has arisen in porous metals as synthetic support for bone integration and regeneration for the fabrication of orthopaedic and dental implants [3,4].

The main interests for using porous metal comes from the increase of the friction coefficient between the implant and the surrounding bone that provides better initial stability and the fact that the interconnected porosity allows tissue in-growth and integration and better long term stability.

The porous structure also helps in adjusting the mechanical properties of the implant to values close to those of bone in order to provide a better stress transfer to surrounding bone, yielding a better bone-metal interface integrity and bone health in the area surrounding the implant [5].

Different processes have been developed to produce porous surfaces for orthopaedic and dental applications. The most commonly used are sintered beads and fibres and thermal spray coating. During the last few decades, research has focussed on the development of highly porous structure or

foams to obtain materials with properties closer to those of bones, structured for better cell response.

A process has been developed recently to produce highly porous titanium with open porosity [6]. Titanium powder, a solid polymeric binder and a foaming agent are dry-mixed together and moulded into the desired shape. The moulded powder is then heat-treated in a three-step heat cycle including foaming, debinding and sintering. During the foaming step, the binder melts and flows around the metallic particles. Once the binder is liquefied, the foaming agent starts to decompose and generates a gas that expands the material. After the foaming step, the resulting material is a solid polymeric foam charged with metallic particles. The material is then treated at higher temperatures to decompose the

polymer while maintaining the cellular structure of the material.

After debinding, the material is sintered to promote solid-state diffusion and to create metallurgical contacts between the metallic particles that provide mechanical strength to the foam. The process allows the production of materials having different structure, density and pore size. Typical porosity levels range typically between 50 and 65%. The compressive strength and rigidity of these materials may also be adjusted. Their corrosion resistance in simulated body fluids is similar to that of solid titanium [7]. More detailed results on the morphology, properties and characteristics of these titanium foams having different pore sizes could be found elsewhere [8,9,10,11]. Table 1 summarises the typical properties of the titanium foam developed for dental applications.

Table 1. Structural, mechanical and chemical data of Ti foams.

Density (g/cm^3)	1.6-2.25
Porosity (%)	50-65
Pore size (μm)	50-400 μm
Surface Area (m^2/g)	0.05
Oxygen (wt.%)	0.3% (0.24% in solution)
Compressive yield strength (MPa)	25-125
Compressive Elastic modulus (GPa)	5-20

Previous page: Part of the core of an injection moulding die in close up.

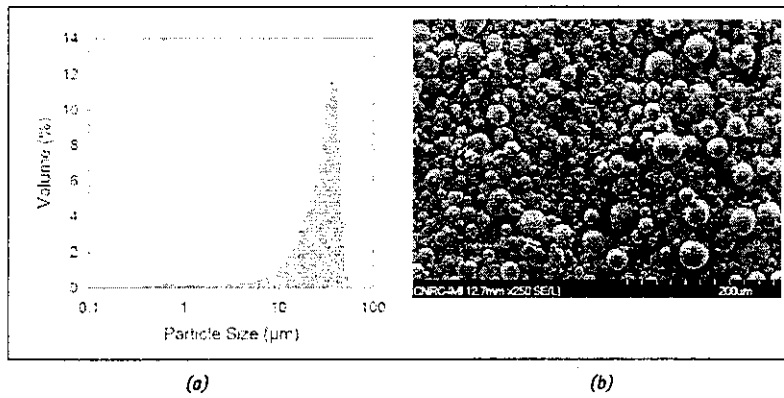


Figure 1. (a) Particle size distribution and (b) SEM micrograph of CpTi powder, Grade 1, <45µm.

The dental implant design needs a dense core in order to permit the fixation of the abutment and crown. The dense core (preform) used in this study is produced by metal injection mould (MIM). This process offers a net-shape method of fabrication of the internal features of the implant which are critical for coupling with the surgeon's tools during the installation of the implant and also with the adjustment of the abutment system. MIM is attractive for its low production costs when compared to the machining route normally used for dental implants.

In the past few years, interest in the development of titanium based components has

risen significantly. Several publications show the progress in Ti and Ti-alloys manufactured by MIM [12,13]. Due to the limited availability of fine titanium powder with low interstitial contents, it is difficult to use powder with particle size normally used in MIM (less than 20 µm). As a result, the powder fraction usually used has a maximum diameter of 45 µm, and this may have a significant effect on dimensional variability. Indeed, Zauner et al. showed that in the green and solvent-debound states, dimensional variability increased with increasing particle size [14].

The powder used in this study was CpTi-Grade 1 (< 45 µm) spherical powder

produced by plasma atomisation (AP&C, Montreal, Canada). Typical size distribution measured by laser diffraction and morphology observed on a scanning electron microscope are shown in Figure 2. Chemical analyses performed using LECO analysers indicate impurity levels of 0.126% of oxygen, 0.009% of nitrogen and 0.005% of carbon. The binder mixture used in this work was composed of polyethylene, paraffin wax and stearic acid.

The feedstock was prepared by mixing 66%vol. of the CpTi powder with the binder components in a planetary mixer using an HV-type blade at 150°C. Injection moulding of the preform of the implant was performed on a Battenfeld Microsystem-50 micro moulding machine at a feedstock temperature of 150°C and a mould temperature of 45°C. A typical production run was composed of 200 parts. The first 20 parts, during process stabilisation, were rejected. Parts were partially debound in hexane at 40°C and the remaining polyethylene was then eliminated during the thermal debinding and pre-sintering performed in purified argon up to 900°C. Parts were finally sintered in a cold-wall vacuum furnace with tungsten heating elements. The sintering was conducted at 1280°C for eight hours with a vacuum of $\sim 10^{-5}$ mbar.

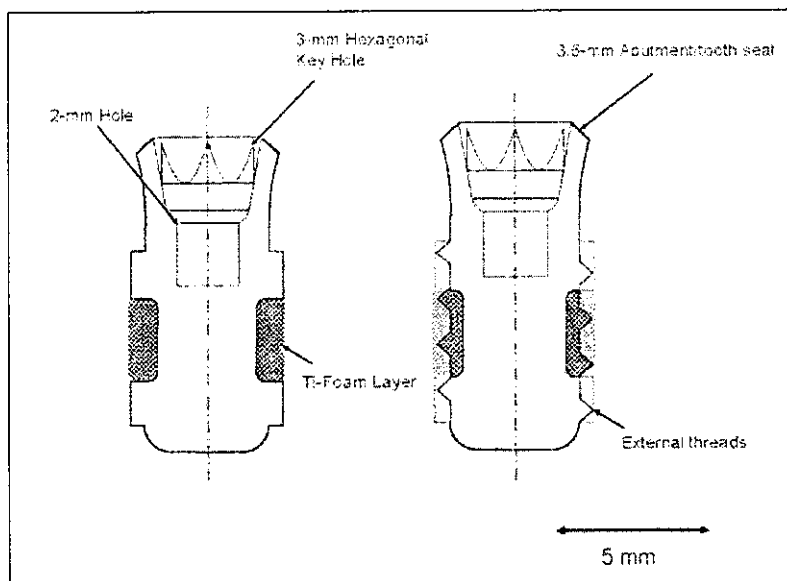


Figure 2. Dental implant design characteristics.

The sintering support was dense yttria (Y_2O_3) plates. Titanium foam was then deposited on the surface of the MIM sintered preforms using the following process [6].

Plasma-atomised CpTi spherical powder ($\sim 180\mu m$, 0.12 wt.% oxygen) was admixed with a polyethylene wax binder in a powder form and a chemical foaming agent

(p,p'-oxybis[benzenesulfonyl hydrazide]). The sintered MIM preforms were inserted in cylindrical molds filled with the powder mixture to produce the foam. The material was then foamed at $210^\circ C$ in air. During foaming, the binder melts and forms a suspension with the other particles. The foaming agent then decomposes and forms a gas that expands the suspension. After foaming, the MIM preforms are covered with a polymeric foam charged with the titanium particles.

Mould design

The foam was then debound at $450^\circ C$ and pre-sintered at $800^\circ C$ in Argon to remove the binder and partially consolidate the titanium particles together and bind the foam to the MIM dense preforms. The threads were then machined in the foam and the specimens were finally sintered at $1400^\circ C$ under vacuum (10^{-5} - 10^{-6} Torr range) to fully consolidate the porous coating.

The dense core shape is illustrated in Figure 2. More than six features are

specified for the internal structure of the implant. The main internal features are the 3.02 mm hexagonal hole for the screw driver tool bit (3 mm hex. key) used by the surgeon and the 2.0 mm internal hole that will be tapped with fine treads for the fixation of the abutment. The 3.50 mm abutment seat diameter is also an important feature of the component. After the final machining of the external threads, the implant is 10.0 mm long with a shank diameter of 4.0 mm.

The mould design was optimised using the NRC-IMI parallel finite element computation modelling software to simulate the process in 3D and predict the behaviour of the feedstock during the mould filling, compacting and cooling phases.

The simulation for a metal injection moulding compound, which is strongly influenced by thermal conditions, predicted several observed flow patterns: initial free surface flow (or jetting) and folding flow to form surface defects [15]. Several gate configurations were proposed initially (see Figure 3) and were validated using the modelling software before machining the

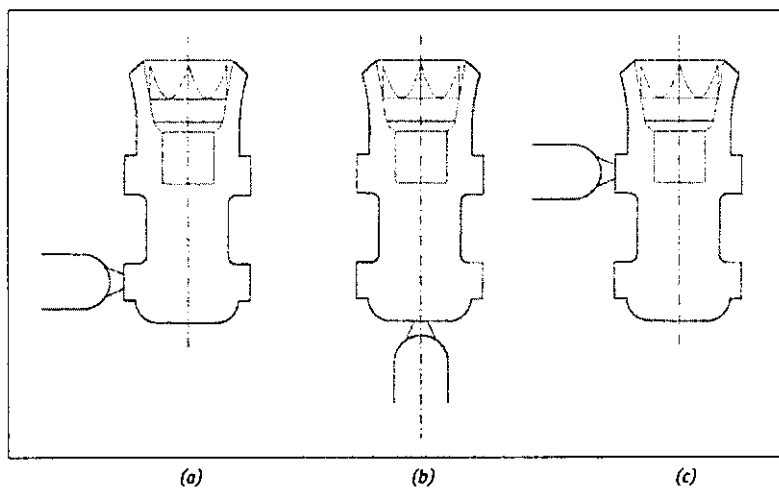


Figure 3. Possible gate configurations.

optimised configuration. Figure 4 shows the die filling simulation of the best gating scenario (Configuration a).

Other gate configurations show important jetting and flow folding (Configuration b) or a weld line in an important load bearing area (Configuration c). The mould cavity was machined according to the

optimal configuration (gate location and dimensions).

Process variability

A sampling of 50 preforms were analysed from the production in order to evaluate the variability of the process.

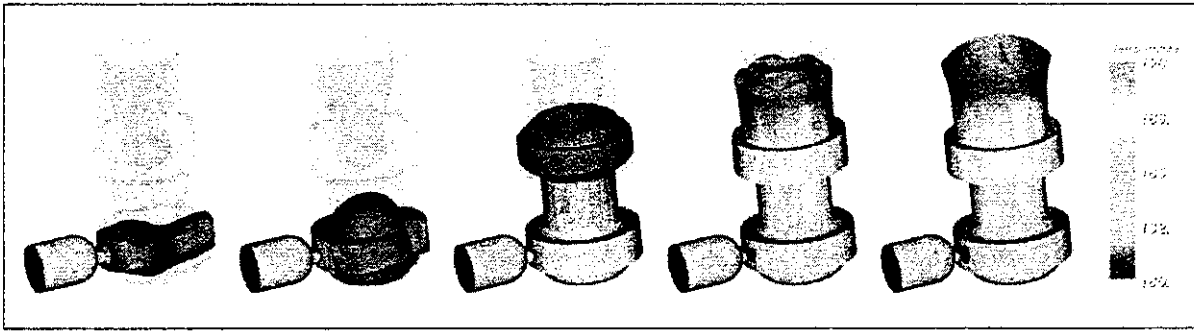


Figure 4. Die filling simulation : 0.02 seconds filling time of the gate configuration (a).

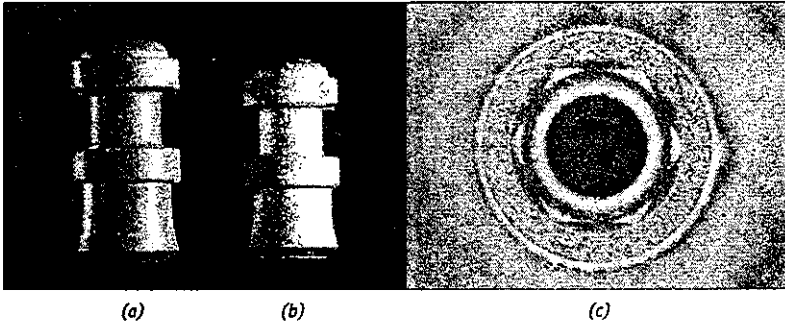


Figure 5. The implant preform (a) as-moulded, (b) sintered states and (c) details of the internal features of the sintered preform.

Figures 5a and 5b show the preform in the as-moulded and as-sintered states and Figure 5c presents a detailed view of the internal features. The average sintered density, measured by gas pycnometry, was $4.40 \pm 0.04 \text{ g/cm}^3$ (i.e. $97.83 \pm 0.95\%$ density). The shrinkage after sintering was 10.90%.

The variability was measured from injection moulding to final sintering. The variations in injected volume and part weight are illustrated in Figure 6 and summarised in Table 2. The injection moulding step shows a coefficient of variation (CV) of 0.0869%, which is the lowest variation measured on all the parameters studied in this work. This indicates a good control of the dosing unit. The as-moulded weight shows a larger variability (0.5402%) that is mainly related to the reproducibility of the runner/part separation. Indeed, it was observed that the gate was breaking below or above the part surface. This effect is significant for small parts less than 500 mg. Despite the fact that this source variability is directly transmitted to the weight variability observed after debinding/pre-sintering and sintering steps, it should not affect the dimensional variability of the internal features. However, it should be noticed that the weight variability after debinding/pre-sintering and the sintering steps were higher than after moulding. After sintering, the variability was 0.6505%. This increase in variability is related to variability of the binder content from part to part. Individual weight losses during debinding/pre-sintering step were also evaluated and gave a mean value of $0.04789 \pm 0.00052 \text{ g}$ for a CV of 1.0858%. The sources of this variability are still under investigation but are expected to come from the variability in the feedstock density and, therefore, variability in parts density. This source of variability will in turn have a strong influence on the dimensional variability of the sintered parts.

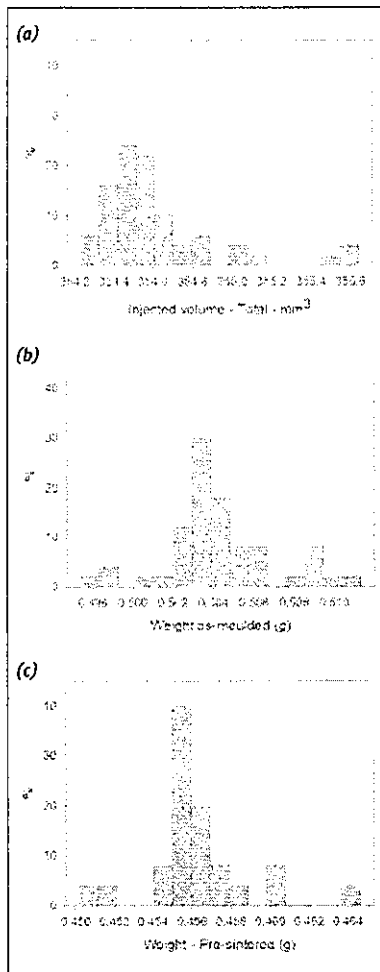


Figure 6. Histogram of the (a) injected volume, (b) as-moulded preform weight and (c) pre-sintered preform weight.

The dimensional variability of two important internal features of the implant was evaluated using a co-ordinates measurement machine (CMM), which has a repeatability of less than 1 µm. The lowest

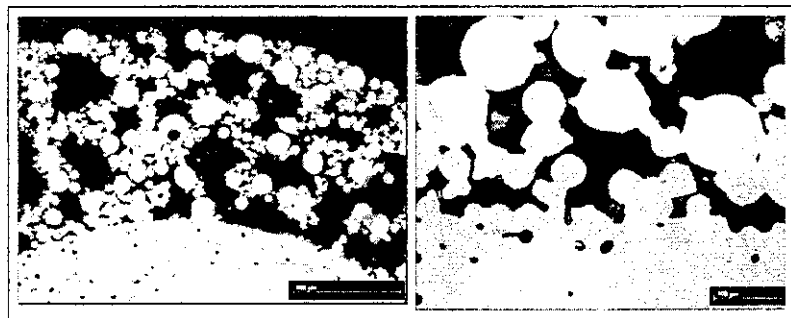


Figure 7. Microstructure of the Ti-foam layer over the dense MIM core.

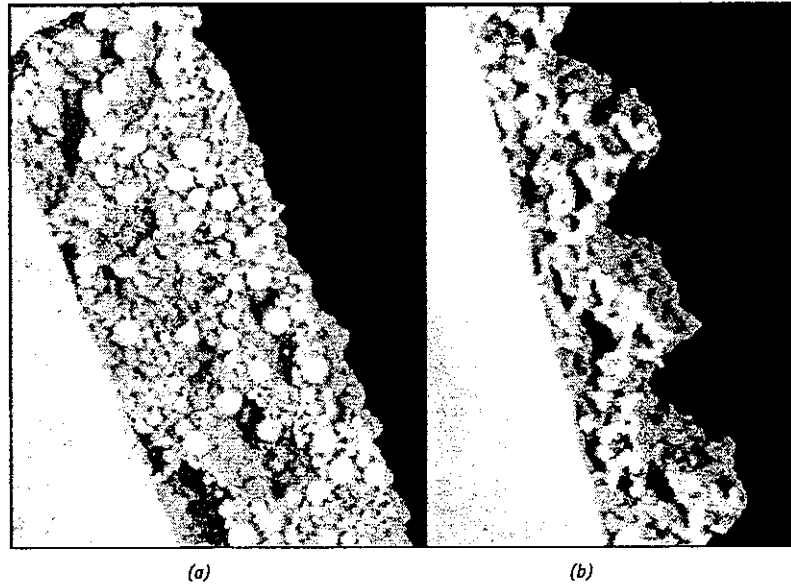


Figure 8. Details of the Ti-foam layer (a) before and (b) after machining of the external threads.

variability was observed on the hexagonal key hole with 0.10220% and 0.41012% for the as-moulded part and the as-sintered part respectively (see Table 2). This means standard deviation (SD) of 3.5 µm, which is

close to reported values []. For the as-sintered dimensions, the standard deviation is 12.4 µm, which is slightly larger than reported values for water atomised 316L stainless steel powders with particle size

	Injected volume (mm ³)	Weight (g)			Abutment/Seat diameter (mm)		Hexagonal key hole (mm)	
		as-moulded	pre-sintered	as-sintered	as-moulded	as-sintered	as-moulded	as-sintered
Mean	354.61	0.5043	0.4562	0.4604	3.9559	3.5253	3.3963	3.0261
Median	354.52	0.5038	0.4556	0.4598	3.9571	3.5260	3.3961	3.0282
S.D.	0.3083	0.002724	0.002730	0.002995	0.00619	0.01625	0.00347	0.01241
C.V. (%)	0.0869	0.5402	0.5984	0.6505	0.15639	0.46118	0.10220	0.41012
Min.	354.23	0.4974	0.4502	0.4578	3.94533	3.5004	3.39108	3.0040
Max.	355.64	0.5113	0.4646	0.4640	3.96257	3.5506	3.40145	3.0389

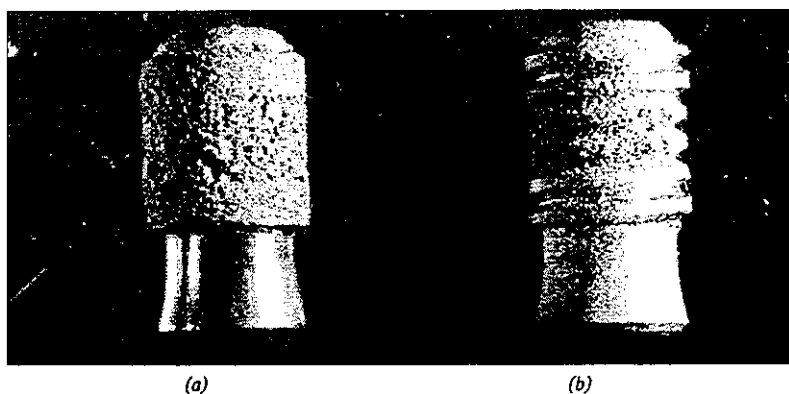


Figure 9. Implant with Ti-foam layer (a) with and (b) without external threads.

distribution smaller than 20 μm . However, in [10], Heaney et al. reported SD of 36.2 μm for sintered component produced with gas atomised powder smaller than 20 μm . The larger variability of the abutment/seat diameter is most likely due to damage of this sharp ridge during handling.

Implant microstructure

The evaluation of the porous/dense implant has not shown increased dimensional variability when compared to the as-sintered preform. The microstructure of the Ti-foam layer is shown in Figure 7. The pore size is typically between 50 and 400 μm and the porosity is interconnected. Sintering necks were formed during sintering and metallurgical bonds were formed between the foam and the dense titanium core. As shown in Figure 8, the machining of the threads did not modify the structure of the Ti-foam layer. The surface of the threads still show the open and interconnected porosity needed for bone in-growth and integration and better long term stability of the implant. Microstructural investigation has shown a good porous/dense interface with good metallurgical bonds. The Ti-foam layer showed an excellent strength and machinability without any closure of the porosity or delamination.

The surface finish of the dense MIM core can be modified in a secondary operation (polishing) in order to match the application requirement (see Figure 9). Indeed, for certain designs, the collar and the abutment/tooth seat need a polished surface to avoid any interaction with the gum tissue.

References

- [1] Branemark, P I et al. (1983) Osseointegrated titanium fixture in the treatment of edentulousness. *Biomaterials*, Vol. 4, pp. 25-28.
- [2] Kasemo, B (1983) Biocompatibility of titanium implant : surface science aspects. *Journal of Prosthetic Dentistry*, Vol. 49, pp. 832-837.
- [3] Meyle, J et al. (1995) Variation in contact guidance by human cells on microstructured surface. *Journal of Biomedical Materials Research* Vol. 29, pp. 81-88.
- [4] Bachle, M and Kohal, R.J. (2004) A systematic review of the influence of different titanium surface on proliferation, differentiation and protein

- synthesis of osteoblast-like MG63 cells. Clin. Oral Impl. Res. Vol. 15, pp. 683-692.
- [5] Simmons, C A et al. (2001) Mechanical Regulation of Localized and Appositional Bone Formation Around Bone-Interfacing Implants. J. Biomed. Mater. Res. Vol. 55, pp. 63-71.
- [6] Lefebvre, L P and Thomas, Y (2003) Method of Making Open Cell Material. US 6,660,224 B2.
- [7] Menini, R, Dion, M J, So, V, Gauthier, M, Lefebvre, L P (2006) Surface and Corrosion Electrochemical Characterization of Titanium Foams for Implant Applications. J. Elect. Chem. Soc. Vol. 153, pp. B13-B21.
- [8] Cheung, S, Gauthier, M, Lefebvre, L P, Dunbar, M, Filiaggi, M (Accepted for publication) Fibroblastic Interactions with High-Porosity Ti-6Al-4V Metal Foam. Journal of Biomedical Materials Research (B), Applied Biomaterials. Part A.
- [9] Lefebvre, L P, Blouin, A, Rochon, S M, Bureau, M N (2006) Elastic Response of Titanium Foams, During Compression Tests and Under Laser-Ultrasonic Probing. Advanced Engineering Materials. Vol. 8, pp. 841-846.
- [10] St-Pierre, J P, Gauthier, M, Lefebvre, L P, Tabrizian, M. (2005) Three-dimensional growth of differentiating MC3T3-E1 pre-osteoblasts on porous titanium scaffolds. Biomaterials, Vol. 26, pp. 7319-7328.
- [11] Gauthier, M, Lefebvre, L P, Thomas, Y, Bureau, M N (2004) Production of Metallic Foams Having Open Porosity Using a Powder Metallurgy Approach. Materials and Manufacturing Processes, Vol. 19, pp.793-811.
- [12] Limberg, W et al., (2004), Metal injection moulding of an advanced bone screw using Ti6Al7Nb alloy powder. Euro PM 2004 Conference Proceeding, Vol. 4, pp. 457-462.
- [13] Guo, S et al., (2004), Mechanical properties and microstructure of Ti-6Al-4V compacts by metal injection molding. Trans. Nonferrous Met. Soc. China, Vol. 14, pp. 1055-1061.
- [14] Zauner, R et al. (2002) The Effect of Powder Type and Powder Size on Dimensional Variability in PIM. Advances in Powder Metallurgy and Particulate Materials, pp. 10.191-10.198
- [15] Ilinca, F et al. (2002) Metal Injection Molding: 3D Modeling of nonisothermal filling. Polymer Engineering and Science, Vol. 42, pp. 760-770.
- [16] Heaney D et al. (2004) Variability of powder characteristics and their effect on dimensional variability of powder injection moulded components. Powder

The Authors

This article was drawn from *Development of a composite porous/dense titanium dental implant using a MIM preform*, a paper by Eric Baril, Louis-Philippe Lefebvre, Yannig Thomas and Florin Ilinca, who work at The National Research Council of Canada/Industrial Materials Institute, 75 de Mortagne Blvd, Boucherville, J4B 6Y4, Québec, Canada. It was given at EuroPM 2007 in Toulouse.